

This work was written as part of one of the author's official duties as an Employee of the United States Government and is therefore a work of the United States Government. In accordance with 17 U.S.C. 105, no copyright protection is available for such works under U.S. Law.

Public Domain Mark 1.0

<https://creativecommons.org/publicdomain/mark/1.0/>

Access to this work was provided by the University of Maryland, Baltimore County (UMBC) ScholarWorks@UMBC digital repository on the Maryland Shared Open Access (MD-SOAR) platform.

Please provide feedback

Please support the ScholarWorks@UMBC repository by emailing scholarworks-group@umbc.edu and telling us what having access to this work means to you and why it's important to you. Thank you.



Analysis of long-range transboundary transport (LRTT) effect on Korean aerosol pollution during the KORUS-AQ campaign

Seoyoung Lee^a, Jhoon Kim^a, Myungje Choi^{a,b}, Jaemin Hong^a, Hyunkwang Lim^a, Thomas F. Eck^c, Brent N. Holben^c, Joon-Young Ahn^d, Jeongsoo Kim^d, Ja-Ho Koo^{a,*}

^a Department of Atmospheric Sciences, Yonsei University, Seoul, 03722, South Korea

^b Jet Propulsion Laboratory, California Institute of Technology, Pasadena, CA, 91109, USA

^c NASA Goddard Space Flight Center, Greenbelt, MD, 20771, USA

^d National Institute of Environmental Research, Incheon, 22689, South Korea

ARTICLE INFO

Keywords:

KORUS-AQ

Long-range transboundary transport

AOD

GOCI

AERONET

ABSTRACT

We investigated the influence of long-range transboundary transport (LRTT) on the aerosol concentrations in the Korean peninsula using the ground- and satellite-based remote sensing with back-trajectory calculations during the Korea-United States Air Quality (KORUS-AQ) campaign. Specifically, aerosol optical depth (AOD) observations from a geostationary satellite can directly provide the progression and evolution of aerosol plume transport. During high pollution cases in western Korea, we found the AOD enhancement over the Yellow Sea and east-central China, at maximum > 200% over the pathway of LRTT compared to the mean condition. Particularly, high AOD in the Shandong peninsula appears coincidentally with the high AOD over South Korea in a day, revealing the strong influence of the east-central Chinese emission. Back-trajectory patterns remarkably capture the movement of high AOD bands detected by the geostationary satellite monitoring. LRTT cases through the inside of boundary layer at east-central China usually contribute to the high AOD in Korea, while air-masses above the boundary layer in north China and Mongolia do not much relate to the Korean pollution, showing the importance for both the direction and height of the air-mass movement. Travel speed is another significant factor to describe the LRTT effect. Despite the large effect of LRTT to both urban and rural sites in Korea, sometimes urban sites are more affected by the domestic emission when the air-mass travels shorter than ~ 250 km per day, notifying that the effect of Korean domestic emission cannot be negligible as well. Our findings reveal that usage of geostationary satellite observations enables us to better evaluate the influence of LRTT on the local air pollution.

1. Introduction

Korean air quality sometimes becomes inferior under particular meteorological conditions when severe air pollution occurs in China and drifts eastward, because Korea is often located in downwind region (Lee et al., 2013a; Seo et al., 2017). Since it is not easy to control the emission and production of air pollutants over external areas, the cause and effect of long-range transport to the Korean peninsula should be evaluated in detail to help in coping with these problematic air quality issues.

Several previous studies have investigated the pattern of air-mass transport to improve understanding of the spatiotemporal features of aerosol pollution in the Korean peninsula. Back-trajectory modelling is a general approach to estimate the potential source regions of air-mass

transport, therefore it has been utilized frequently in combination with the measurement of regional aerosol concentration. Since the National Institute of Environmental Research (NIER) of the South Korea government has monitored surface particulate matter (PM) since the early 2000s (Yoo et al., 2015), some previous back-trajectory analyses were conducted to explain where the source of polluted air-masses originate, associated with increased PM (Choi et al., 2014; Oh et al., 2015). These back-trajectory analyses have been also used to identify possible source locations for chemical compositions of PM (He et al., 2003; Sahu et al., 2009). In addition, a number of statistical approaches have also been used such as potential source contribution function (PSCF) method and concentration weighted trajectory (CWT) model (Heo et al., 2009; Jeong et al., 2011, 2017).

However, sometimes the long-range transboundary transport

* Corresponding author. Dept. of Atmospheric Sciences, Yonsei University, 50 Yonsei-ro, Seodaemun-gu, Seoul, 03722, South Korea.

E-mail address: zach45@yonsei.ac.kr (J.-H. Koo).

<https://doi.org/10.1016/j.atmosenv.2019.02.020>

Received 16 September 2018; Received in revised form 16 January 2019; Accepted 10 February 2019

Available online 19 February 2019

1352-2310/© 2019 Elsevier Ltd. All rights reserved.

(LRTT) occurs above the boundary layer (Yu et al., 2008), which may not be measured by surface monitoring. Thus, analyses based on surface observations alone have some limitations to diagnose the pattern of LRTT. For this reason, many previous works used column integrated information such as aerosol optical depth (AOD). Based on the ground-based AOD measurements at Aerosol Robotic Network (AERONET; Holben et al., 1998) or Skyradiometer Network (SKYNET; Nakajima et al., 1996) sites, calculated back-trajectories have been investigated to find the source region of polluted air masses contributing to the high air turbidity over the Korean peninsula (Lee et al., 2006, 2018a; Kim et al., 2012). Additionally, back-trajectory analyses were used to explain aerosol types classified based on the aerosol optical properties (Schmeisser et al., 2017; Lee et al., 2018b). Assimilated AOD information was also considered for this back-trajectory analysis (Park et al., 2014; Saide et al., 2014).

These previous studies achieved some findings enhancing the basic knowledge about the influence of LRTT on the Korean air quality. At least, it can be stated that the air-mass transport from the polluted regions in China frequently coincides with high air pollution levels in South Korea (Kim et al., 2009; Lee et al., 2011). Nevertheless, these findings have been debatable because the back-trajectory information does not always clearly illustrate the movement of real polluted air masses. In other words, the interpretation of back-trajectories only can be accepted as an indirect clue to describe the AOD variation observed at the Eulerian ground station. Since the on-site emission and local production of air pollutants can be another important source of regional pollution, it is difficult to corroborate the LRTT effect or quantify the full influence of LRTT based on the only back-trajectory analysis. The Lagrangian style approach such as from aircraft observations can follow the movement of air parcels, but it hardly supports the goal of continuous monitoring.

Satellite measurements are good approach to get over mentioned issues. Several previous studies have investigated the transport effect of air pollutants originated from China using the lower Earth orbit (LEO) sensors such as the Ozone Monitoring Instrument (OMI), Moderate Resolution Imaging Spectroradiometer (MODIS) and Cloud-Aerosol Lidar with Orthogonal Polarization (CALIOP) (Eguchi et al., 2009; Guo et al., 2010, 2017; Yu et al., 2008; Yumimoto et al., 2010). In spite of the large contribution to the analysis of long-range transport such as the trans-Pacific transport, studies using LEO measurements still have a limitation for capturing the detail properties of transboundary transport due to their temporally coarse coverage (e.g., once a day). In contrast to the LEO satellite, geostationary satellite imagery with better temporal resolution can detect the highly variable movement of real pollutants over the target domain, which typically includes the continental scale. Thus, the geostationary satellite measurements can be a good solution to see the aerosol plume transport between countries and/or regions. Actually, AOD measurements over East Asia have been performed since ~2010s using the Geostationary Ocean Colour Imager (GOCI) and meteorological imager (MI) onboard the Communication, Ocean, and Meteorology Satellite (COMS) satellite (Choi et al., 2016; Kim et al., 2016), and Advanced Himawari Imager (AHI) onboard the Himawari-8 satellite (Lim et al., 2018). These satellite missions provide AOD products once per hour or better, which guarantee the high temporal resolution monitoring. Therefore, the usage of these high frequency AOD values will enable more rigorous analysis for the evaluation of LRTT effect on the air quality in Korea.

Given this motivation, in this study we investigate the characteristics of LRTT during the Korea-United States Air Quality (KORUS-AQ) campaign executed from 1 May to 12 June 2016 over and around the Korean peninsula. Since the AOD over the Korean peninsula usually shows the highest value in this period, particularly in June (Kim et al., 2007; Koo, 2008), Evaluating the contribution to the local high turbidity is one of the important issues for the Korean society. Multiple data from the ground- and satellite-based remote sensing measurements are utilized and examined along with back-trajectory calculations. In

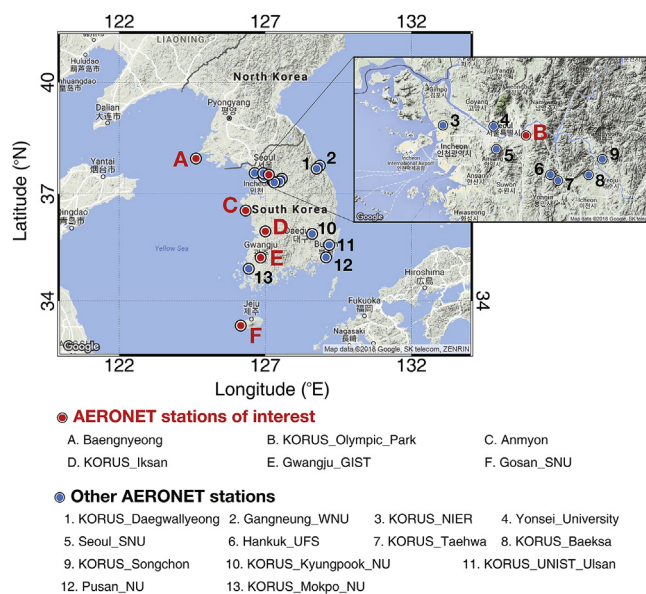


Fig. 1. Locations of AERONET sites in the Korean peninsula during the KORUS-AQ campaign.

particular, direct application of geostationary satellite observations is an important step in this study. Based on these data, we compared cases for high and low aerosol concentrations to find out the main pathway of LRTT and the enhanced level of air pollution when the substantial amounts of aerosols are observed in South Korea. Furthermore, we examine how the geometry of LRTT relates to the extent of aerosol pollution, and evaluate the contribution of potential source regions to the air turbidity in Korea. Individual findings at each ground-based station are also compared to see the regional difference of LRTT effect.

2. Data description

During the KORUS-AQ campaign from 1 May to 12 June in 2016, aerosol optical properties were obtained from 19 AERONET Sun-sky radiometer sites located in the Korean peninsula (Fig. 1), and also from GOCI satellite measurements over the extended region. In addition to these aerosol optical properties, regional meteorology and back-trajectories are utilized for the analysis in this study.

2.1. AERONET measurements

AERONET, a global ground-based remote sensing network, provides aerosol optical properties using sun-sky radiometer measurements (Holben et al., 1998). These data have been widely used for the analysis of regional aerosol characteristics and the validation of satellite retrievals, due to the high accuracy of measured AOD. The estimated uncertainty of AERONET AOD is mainly attributed to the calibration uncertainty (about 0.010–0.021 for field instruments), and errors become high in the ultraviolet wavelengths (Eck et al., 1999).

AERONET data are available at the three data quality levels: Level 1.0, Level 1.5, and Level 2.0. Level 1.5 AOD values are near-real time data produced by applying the cloud screening process (Smirnov et al., 2000) to unscreened data (Level 1.0). Level 2.0 data are the final quality assured products applying post field calibration, usually examined for data analysis. Also, the version of AERONET data is divided in accordance with the cloud screening, quality control screening and the retrieval algorithms; Versions 2 and 3 are generally used. Recently, AERONET version 3 data are newly released with several improvements compared to version 2, particularly in cloud screening procedure based on the temporal variability of AOD (Eck et al., 2018; Giles et al., 2019). According to Eck et al. (2018), AERONET version 3 can preserve high

AODs for fine mode dominated cases, which were considered as cloud and sometimes eliminated in version 2 dataset. In this study, we mainly employ the level 2.0 version 3 data for the analysis, but also adjunctively examine version 2 data for the comparison purpose.

During the KORUS-AQ campaign, AERONET monitoring sites (Fig. 1) were located in both urban (e.g., Olympic Park) and rural areas (e.g., Baengnyeong), therefore the comparison between the trans-boundary transport and local emission is possible. Also, most of these stations are located in the western part of the Korean peninsula, beneficial for looking into the transport of air pollutants over the Yellow Sea. Assuming that these west coastal sites are significantly under the direct influence of air-mass transport from the west, we select six target sites for detailed analyses: Baengnyeong (37.97°N, 124.63°E), KORUS_Olympic_park (37.52°N, 127.12°E, hereafter Olympic Park), Anmyon (36.54°N, 126.33°E), KORUS_Iksan (35.97°N, 127.00°E, hereafter Iksan), Gwangju_GIST (35.23°N, 126.84°E, hereafter Gwangju), and Gosan_SNU (33.29°N, 126.16°E, hereafter Gosan).

In this study, we mainly used the AOD at 500 nm and Ångström Exponent between 440 and 870 nm (AE) as the primary parameters for the monitoring of regional aerosol properties. AOD is the parameter showing the atmospheric turbidity induced by the radiative absorption and especially scattering of aerosols. AE indicates the spectral variation of AOD, defined as the slope of linear regression between AOD and wavelength in a logarithmic scale. This AE is generally considered as a proxy of particle size (e.g., Eck et al., 1999). At all AERONET sites, AOD and AE are obtained using the Direct Sun measurements at seven channels (340, 380, 440, 500, 675, 870, and 1020 nm), while only a subset of these AOD is utilized in this study.

2.2. GOCI YAER version 2 data

The GOCI instrument onboard the COMS is the world's first ocean colour imager in geostationary orbit (Choi et al., 2012). GOCI covers 2500 km × 2500 km area centered at 130° E, 36° N with high spatial resolution (500 m × 500 m). The spectral channels of GOCI include 6 visible (412, 443, 490, 555, 660, and 680 nm) and 2 near-infrared (745 and 865 nm) bands. Since 2011, the GOCI mission has produced an hourly interval dataset from 00:30 to 07:30 UTC (09:30 to 16:30 Korean Standard Time) every day. Based on this dataset with the GOCI Yonsei aerosol retrieval (YAER) algorithm, hourly aerosol optical properties are retrieved from the eight spectral channels (Choi et al., 2016, 2018). While the LEO satellite measurements such as the MODIS has a temporal limitation for the monitoring of regional air conditions (generally performed once a day), analysis based on GOCI products can detect the continuous movement of airborne aerosols, which is more useful to investigate the development, transport and evolution of aerosol plumes.

Since clouds strongly interfere with the radiative signals related to the detection of airborne aerosol, cloud screening is an essential process when we attempt to retrieve accurate aerosol optical properties using the satellite remote sensing measurements. To reduce the effects of cloud contamination, several cloud masking techniques are applied to the GOCI YAER algorithm (Choi et al., 2018). After screening clouds, the remaining pixels are aggregated to a pixel with a spatial resolution of 6 km to enhance the signal of aerosols. At this point, the process removing the brightest 40% and darkest 20% of pixels is also performed to eliminate the effects of the remaining clouds, cloud shadow and surface contamination. Owing to the absence of thermal infrared channels which are sensitive to the presence of clouds, however, cloud contamination can remain and cause positive biases in GOCI AOD compared to AERONET AOD (Choi et al., 2018). Therefore, the cloud mask at 6 km resolution in the AHI YAER algorithm (Lim et al., 2018) using infrared channels is additionally applied to the GOCI AOD. In this study, GOCI AODs at 550 nm with 6 km resolution are basically used, but also reconstructed $0.2^\circ \times 0.2^\circ$ grid AOD data are exploited when more averaged patterns are interests. For the validation purpose, we

compare the pattern of GOCI AOD with that of AHI and MODIS AOD.

2.3. Backward trajectories and meteorological data

To evaluate the spatiotemporal patterns of air mass transport, the backward trajectory (hereafter back-trajectory) is calculated using the Hybrid Single Particle Lagrangian Integrated Trajectory (HYSPPLIT) model version 4.0 (Stein et al., 2015) developed by National Oceanic and Atmospheric Administration (NOAA) Air Resources Laboratory (ARL). For the meteorology in the back-trajectory calculation, we use the dataset of global data assimilation system (GDAS) with $1^\circ \times 1^\circ$ resolution provided from the National Centers for Environmental Prediction (NCEP). To more underline the influence of adjacent emission sources, 2-day back-trajectories arrived at 500 m above ground level are computed every hour during the whole KORUS-AQ campaign for each AERONET station. Compared to the back-trajectory pattern, we also examine the meteorology field using the European Centre for Medium-Range Weather Forecasts (ECMWF) ERA5 and NCEP & National Centre for Atmospheric Research (NCAR) reanalysis dataset.

3. Results and discussions

We first look at the temporal variation of AOD and AE obtained from the AERONET measurements in South Korea during the KORUS-AQ campaign. Fig. 2 illustrates the variation of daily mean AODs at 550 nm and AE at 440–870 nm in the sequence of latitudes: from Baengnyeong, the highest latitude site (37.97°N), to Gosan, the lowest latitude site (33.29°N). Here we investigate the AERONET version 3 products, which are recently updated based on the new algorithm improving the detection of fine mode particles (Eck et al., 2018), but confirm that analyzed results based on version 2 products are analogous (Fig. S1). In general, the middle range of sites in South Korea often shows high AODs. From this figure, we can find 3 representative cases showing the high AOD: 25–26 May (case 1), 30–31 May (case 2), and 7–8 June (case 3). AE values are ~ 1.0 during these cases, implying the large contribution of fine-mode particles to high aerosol pollution, supported by the pattern of fine mode fraction from the AERONET data set (Fig. S2).

Hourly AOD images from the GOCI satellite measurement can show the progression of aerosol plumes for these 3 high AOD cases (Figs. S3, S4, S5, S6, S7, and S8). Daily mean AOD distribution, which is produced using hourly AOD images, more obviously indicates that 3 high AOD cases are attributed to the aerosol transport from China (Fig. 3). Himawari-8 AHI AOD also shows the similar spatial pattern (Fig. S9). Comparing these geostationary AODs with the AOD distribution obtained from the LEO satellites, such as MODIS onboard Aqua and Terra satellites (Figs. S10 and S11), we can notice that the geostationary observations provide much improved scene of regional AOD patterns. Since the bright sun glint pixels for MODIS are often located over the Yellow Sea and East Sea (Choi et al., 2018), there is a difficulty for analysing and detecting the aerosol plumes transported to the Korean peninsula. Although LEO satellite AOD measurement has somewhat contributed to the understanding of the regional transport pattern in South Korea (Lee et al., 2006; Kim, 2008), this limitation of LEO satellite data is undeniable, revealing the necessity of geostationary satellite monitoring (Naeger et al., 2016).

As shown in Fig. 3, mostly heavy aerosol plumes appear to be generated in east-central China particularly in the Shandong peninsula and subsequently advected across the Yellow Sea. Finally, this heavy aerosol plume passes over the middle to northern part of South Korea, coincided with the high AODs in Korea (Fig. 2). Apparently, the effect of LRTT seems important in explaining the total air turbidity over South Korea. Therefore, we first focus on the examination of the difference between the high and low AOD cases to assess whether the LRTT effect is really associated with the severity of high AOD in Korea. Then more general analysis will be continued for the diagnosis of regional

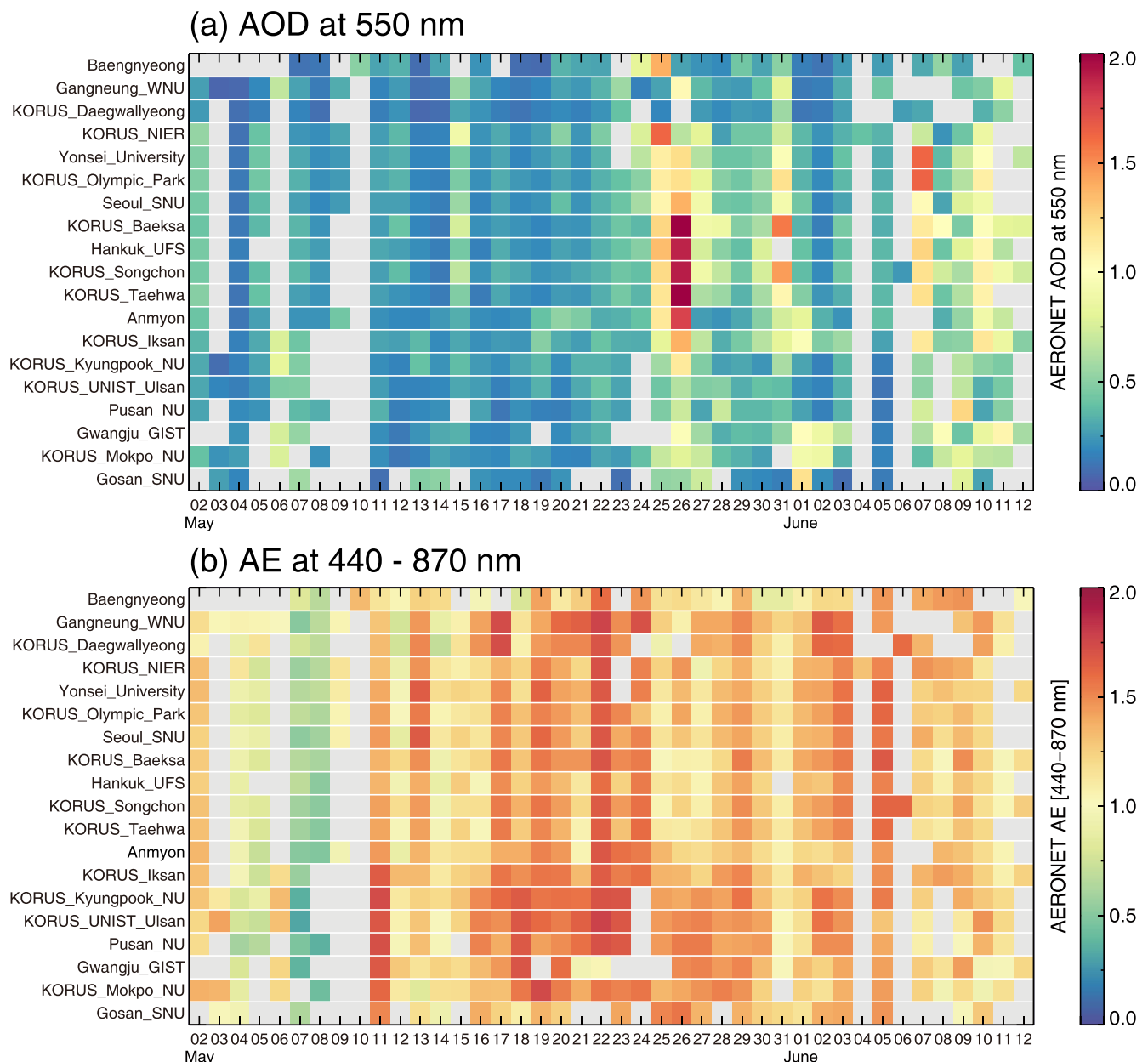


Fig. 2. Daily mean patterns of (a) AOD at 550 nm and (b) AE at 440–870 nm from all AERONET sites in the Korean peninsula during the KORUS-AQ campaign.

characteristics about the influence of the LRTT.

3.1. Comparison of extremely high or low AOD cases

As mentioned, we first try to compare atmospheric situations between high and low AOD cases at 6 target AERONET sites located on the west coastal region of the Korean peninsula. To perform this analysis, we define the extremely high and low AOD case during the campaign by selecting 5 days showing the highest and lowest AODs individually for each site. Selected days for the highest and lowest AOD are summarized in Fig. S12. Mostly high AOD cases are selected from the 3 LRTT periods found in Fig. 3. The middle part of May (11–23 May) exhibited quite low AODs. If there are some differences between these two opposite cases (high and low AOD), the extreme case comparison can inform us about the key processes inducing high atmospheric turbidity in South Korea.

Fig. 4 reveals the East Asian composite images of GOCI retrieved AODs and ECMWF wind vectors for the 5 highest AOD days at the 6

target sites. Application of time lag analysis is useful in considering the duration of air-mass transport. In addition to the composite for the selected high AOD days (hereafter D-0), therefore another composite is also generated using AODs for one day before the selected cases (hereafter D-1). For the high AOD cases at Baengnyeong, Olympic Park, and Anmyon, GOCI D-0 composites clearly indicate the existence of heavy aerosol plumes over the Yellow Sea advected from east-central China. At this point, westerly is also developed over the Yellow Sea. In other words, LRTT directly carries heavy aerosol plumes into Korea when we experience the extremely turbid air conditions at these sites. GOCI D-1 composites also depict the step of aerosol plume evolution, implying that the duration of LRTT can be longer a day. This time lag analysis of plume transport is more apparent at Iksan, Gwangju, and Gosan sites, as the GOCI D-0 composites describe the weaker band of heavy aerosol plume over the Yellow Sea. However, GOCI D-1 composites show rather strong LRTT of aerosol plumes, showing the delay of LRTT influence to the Iksan, Gwangju, and Gosan sites. Perhaps this feature appears because these sites are located in the southern part of

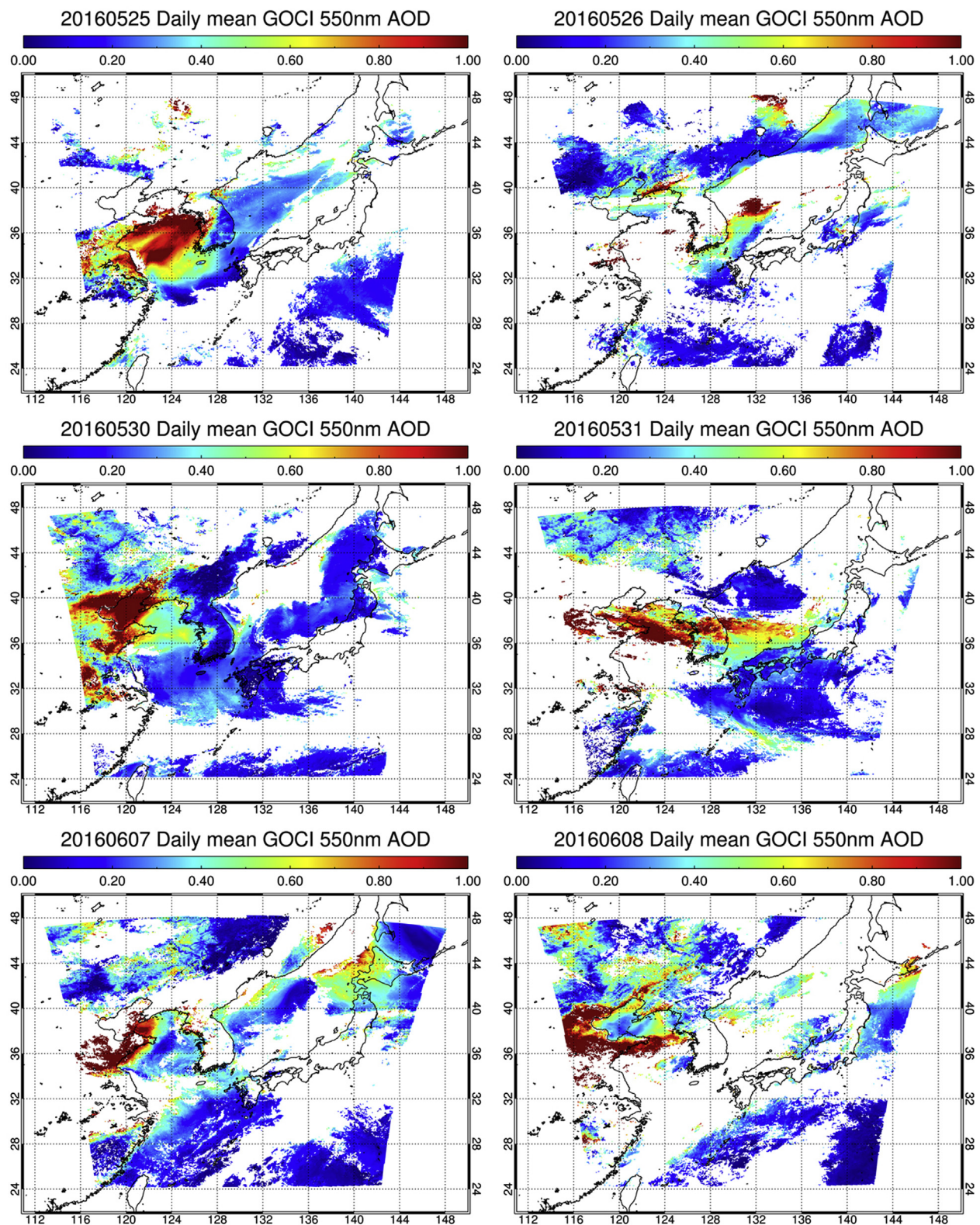


Fig. 3. Daily representative images of GOCI AOD at 550 nm for three example periods: 25–26 May (top), 30–31 May (middle), and 7–8 June (bottom).

the Korean peninsula, a little farther from the emission source regions in China, but also possibly due to latitudinal differences in meteorology, especially wind speed and direction.

In contrast, GOCI AOD composites for 5 lowest turbid days (Fig. 5) do not describe the evolution and progress of LRTT over the Yellow Sea. Particularly AOD values over east-central China including the

Shandong peninsula are quite low. This differs from the high values of AOD over the Shandong peninsula for high turbid cases in Korea (Fig. 4). Spatial distribution of AOD over China should be random regardless of AOD values in South Korea if the effect of transboundary transport is negligible. But geostationary satellite observations detect the huge contrast of AODs over China, proportional to the extent and

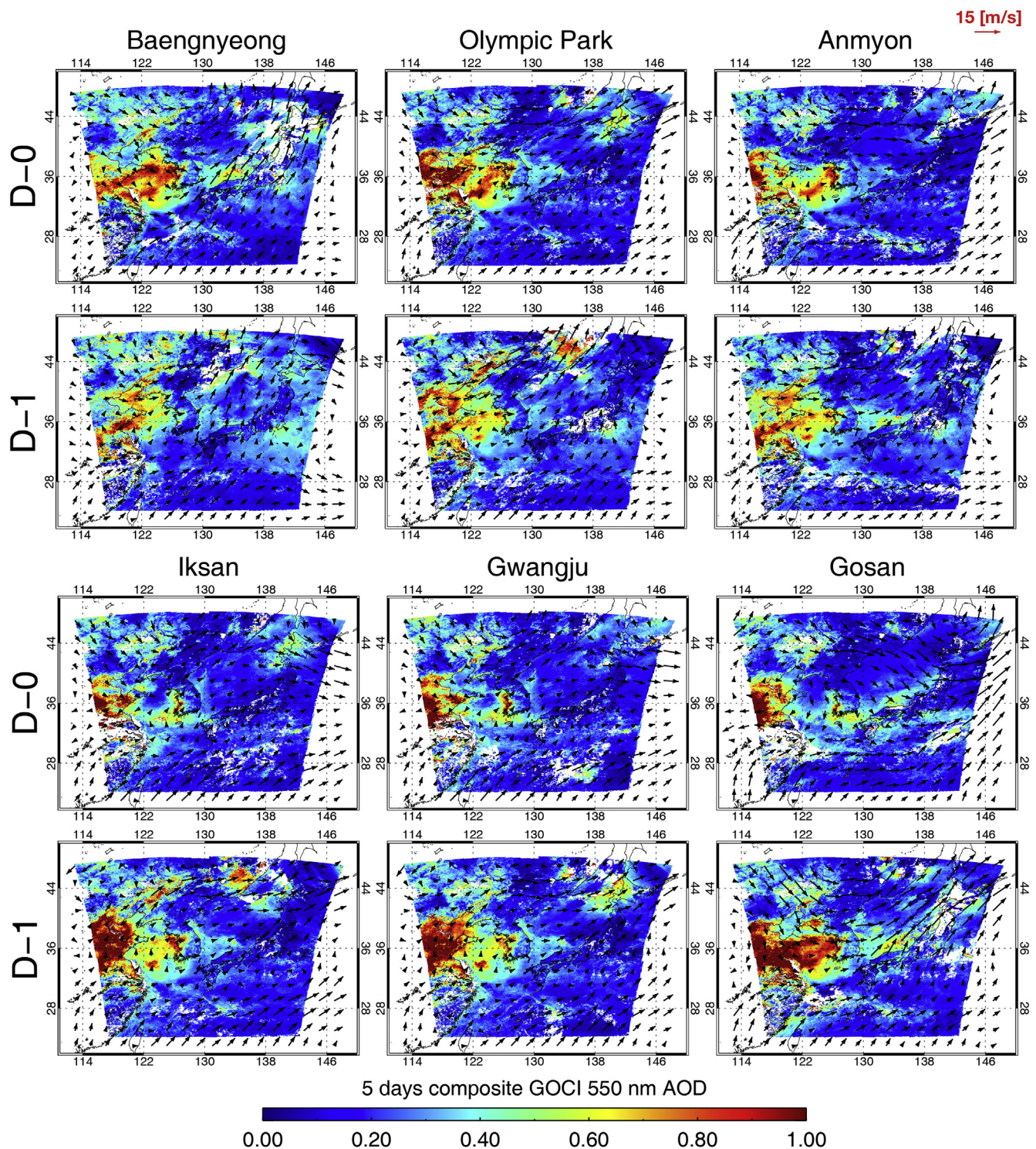


Fig. 4. GOCI AOD (colour contour) composites and wind vectors (black arrow) at 850-hPa pressure level for the 5 highest AOD days at Baengnyeong, Olympic Park, Anmyon, Iksan, Gwangju, and Gosan sites. D-0 means the composite average for selected dates, and D-1 means the composite average for dates of one day before selected dates. (For interpretation of the references to colour in this figure legend, the reader is referred to the Web version of this article.)

magnitudes of AOD in Korea. This finding is obvious evidence showing that air pollutants generated from east-central China contribute to the high AOD over the Korean peninsula.

Since the comparison between the high and low AOD cases clarifies the important role of LRTT, we further quantify the AOD enhancement over the route of LRTT when we observed high AOD conditions in Korea. For the pure evaluation of LRTT effect far from the local continental emission, we estimate the relative difference of AOD over the

Yellow Sea between the highest turbid cases and mean condition during the whole campaign (Fig. 6). Comparing to the mean condition, AOD can be increased by > 200% at maximum due to the LRTT from east-central China. This figure also shows where the AOD is really enhanced: i.e., the pathway of the transported aerosol plume. For example, the high AOD at Baengnyeong results from the direct aerosol plume from the Shandong peninsula, and the high AOD at other sites is dominantly affected by aerosol plumes from the region around Shanghai.

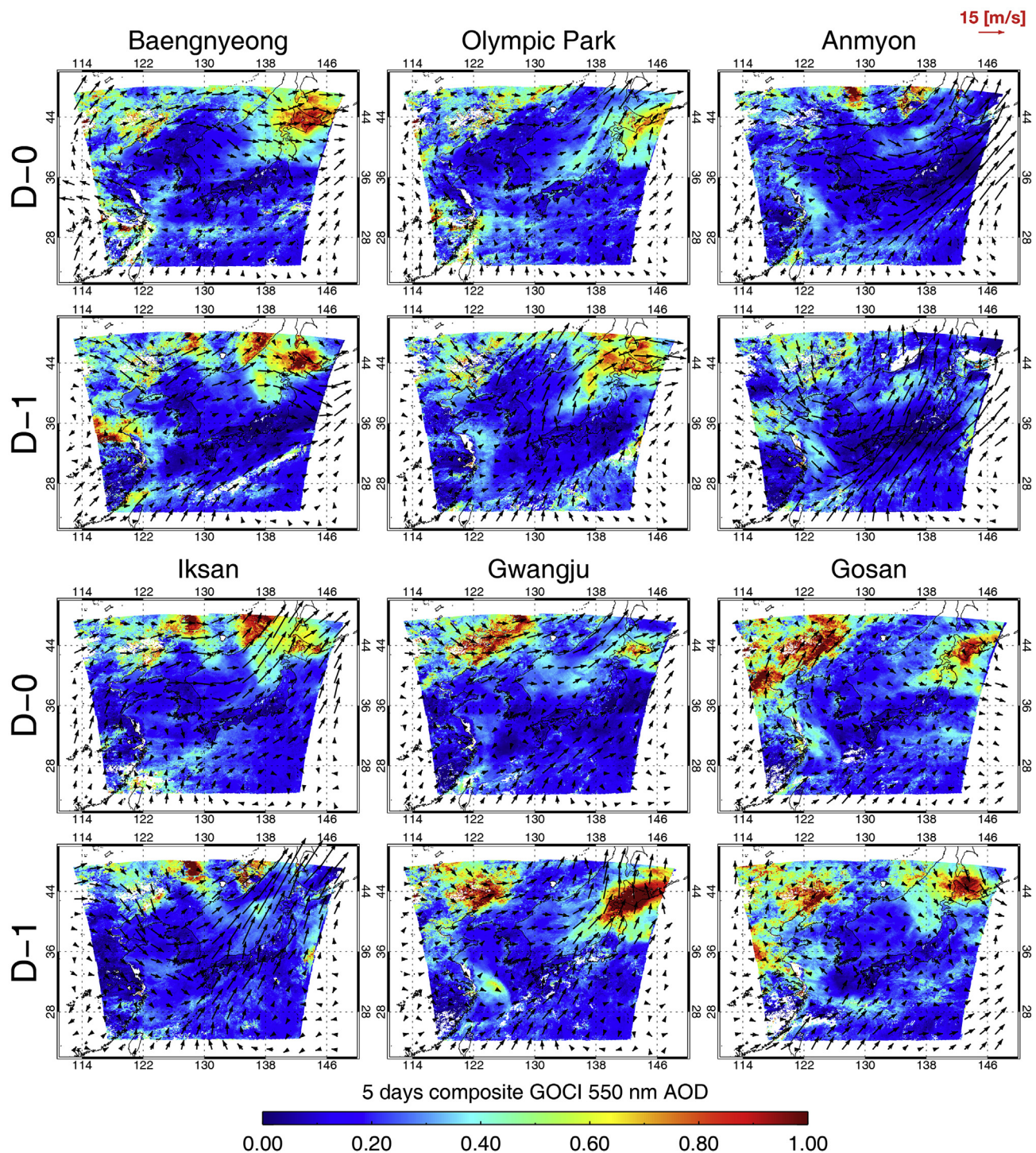


Fig. 5. GOCI AOD (colour contour) composites and wind vectors (black arrow) at 850-hPa pressure level for the 5 lowest AOD days at Baengnyeong, Olympic Park, Anmyon, Iksan, Gwangju, and Gosan sites. D-0 means the composite average for selected dates, and D-1 means the composite average for dates of one day before selected dates. (For interpretation of the references to colour in this figure legend, the reader is referred to the Web version of this article.)

Considering a one-day time lag (D-1), moderate AOD increases near the Beijing-Tianjin-Hebei (BTH) region are also associated with high AOD in South Korea. These analyses of AOD composites seem to indicate where the transport of polluted air masses start and pass through.

We next try to find the spatial pattern of LRTT using 2-day back-trajectories calculated hourly at 6 target sites. Similarly, back-trajectory patterns are compared between the 5 highest and lowest AOD cases (Fig. 7). All 6 target sites indicate the obvious pathway of LRTT during the highest AOD cases; most of the back-trajectories come from east-

central China, pass through the Yellow Sea, and move onto the western coast of Korea. At Baengnyeong and Olympic Park, transported air masses seem to originate from the emission at the Shandong peninsula dominantly. Back-trajectories arrived at other sites which are located somewhat southward, are attributed to the south region of the Shandong peninsula. We additionally find that there is a partial contribution of the BTH region to Gwangju and Gosan sites.

Here we also look at the height variation of back-trajectories. Clearly, the height is maintained in the boundary layer ($< \sim 1$ km)

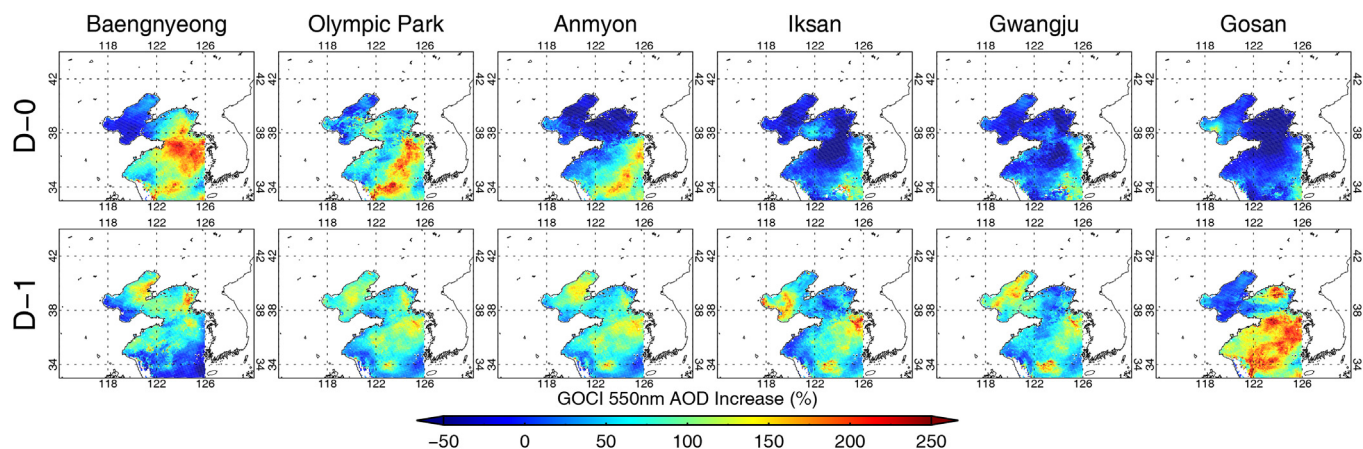


Fig. 6. Relative percentage difference between the mean GOCI AOD for the 5 highest AOD days and mean GOCI AOD for the whole KORUS-AQ campaign (i.e., mean AOD for days of the highest AOD – mean AOD for the whole KORUS-AQ campaign) at Baengnyeong, Olympic Park, Anmyon, Iksan, Gwangju, and Gosan sites. D-0 cases (top) and D-1 cases (bottom) are compared.

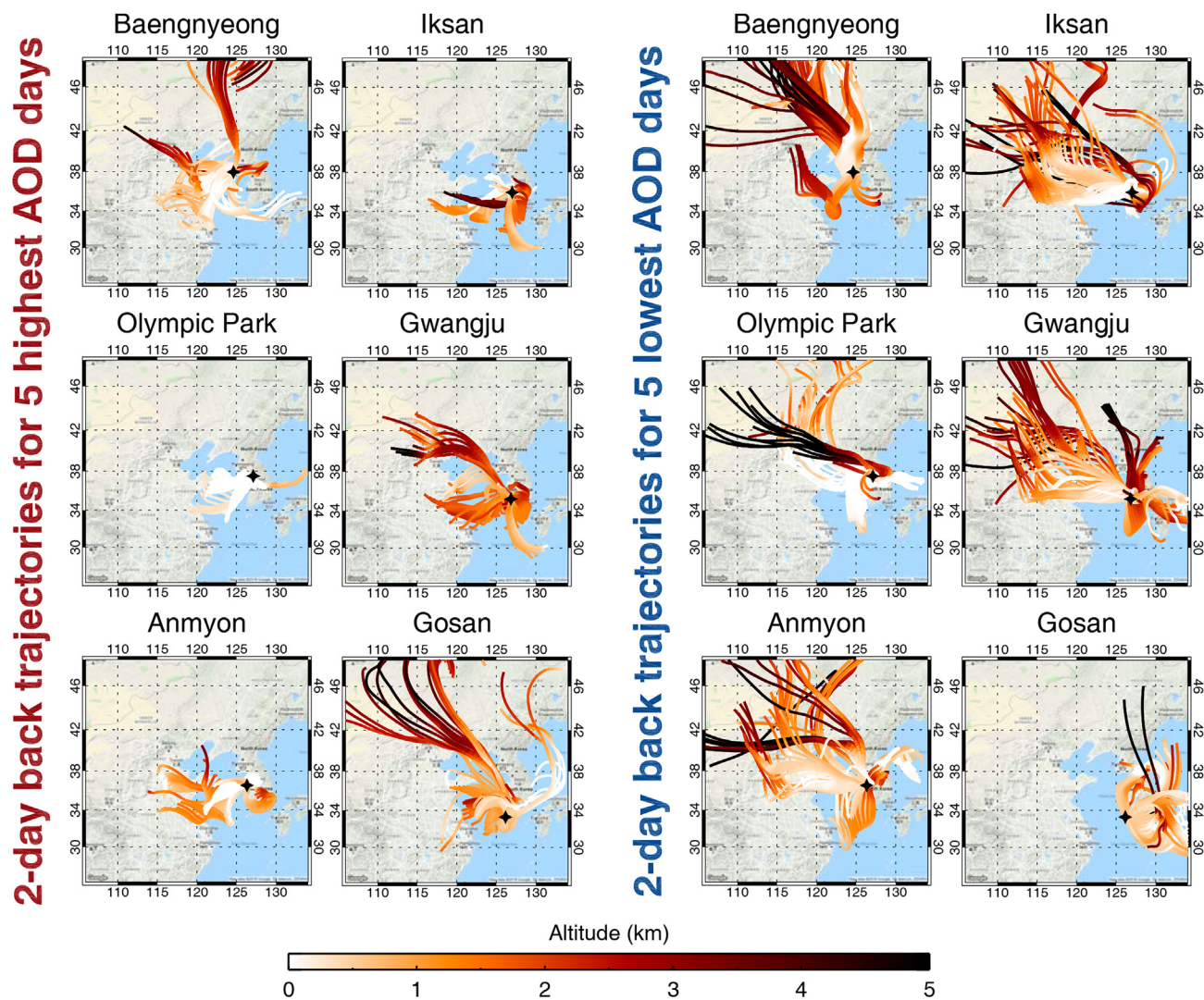


Fig. 7. 2-day back-trajectories obtained from the HYSPLIT-4 simulations for the five highest AOD days and five lowest AOD days at Baengnyeong, Olympic Park, Anmyon, Iksan, Gwangju, and Gosan sites. Different colours indicate the height variation of each back-trajectory. (For interpretation of the references to colour in this figure legend, the reader is referred to the Web version of this article.)

when the air masses come from the Shandong peninsula, indicating that it is highly possible to see the direct intrusion of surface aerosols from China to Korea. When the air masses come from North China or Inner Mongolia, however, the height of back-trajectories is above the boundary layer, which is less polluted. Thus, the transport effect from these regions is relatively weaker, consistent with the findings in Figs. 4–6. Fig. 7 well illustrates that the occurrence of LRTT in the boundary layer is greater when the Korean local AOD is enhanced.

Back-trajectory patterns for the lowest AOD cases are much different in general. Baengnyeong and Olympic Park do not have back-trajectories originating from east-central China much, and. Although some back-trajectories arrived at Anmyon, Iksan, and Gwangju were partially advected from east-central China, we find the significant difference of back-trajectory between the highest and lowest AOD cases in terms of the distance of transport. 2-day back-trajectories for the highest AOD cases look shorter, indicating slower eastward movement. Therefore, most of the back-trajectories stay over the Yellow sea and east-central China. But 2-day back-trajectories for the lowest AOD cases generally indicate more rapid transport from North China and even Mongolia. Although air masses sometimes pass over east-central China, it is likely that the pollution extent in transported air masses is much diluted due to fast wind speed. The lesson from this result is that the transport speed should also be considered to evaluate the LRTT effect in addition to the transport direction and height from the origin region. We will investigate this issue further in a later section.

Based on these analyses, it seems that the combination of geostationary satellite observations and back-trajectories can elucidate whether our interpretation of the effect of LRTT is reasonable or not. For the highest AOD cases at 6 sites, GOCI D-0 and D-1 AOD composites are generated with overlapping 2-day back-trajectories (Figs. 8 and S13). Back-trajectories that arrived at the Baengnyeong, Olympic Park, and Anmyon sites passes primarily over the heavy aerosol plume over the

Yellow Sea in the D-0 composites (Fig. 8). Particularly the agreement between heavy aerosol plumes and back-trajectories for cases at Olympic Park and Anmyon is remarkable. Back-trajectories that arrived at Iksan and Gwangju are more analogous to composite images of D-1 composites (Fig. S13), indicating a daily delayed effect of LRTT on the southern sites, as discussed in Fig. 4. All findings here reveal that back-trajectories for high AOD cases can detect the same pathway of heavy aerosol plumes as were obtained from the satellite measurements. In other words, the combination of back-trajectory and geostationary satellite AOD is perhaps the best approach for the identification and diagnosis of the LRTT effect.

Since air-mass motions depend on the pattern of regional atmospheric dynamics, we examine if regional meteorology shows variation related to the extent of local pollution. Similar to the analyses above, we examine composite images of 850-hPa geopotential height for the highest or lowest AOD cases at 6 target sites (Fig. S14). Generally, a dipole structure is found over East Asia: low pressure on the north side and high pressure on the south side. Due to the typical counter-clockwise circulation of the northern low pressure and clockwise pattern of the southern high pressure, the zonal westerly winds can be accelerated between these two pressure systems (Koo et al., 2016). We can see that the dipole system between the northern low and southern high pressure is largely intensified for the lowest AOD case (Fig. S14). A trough is also well developed and accompanied with the northern low pressure, promoting zonal movement (Cooper et al., 2004). This feature implies that airborne aerosols emitted from China can be quickly traversed over Korea and transported to the North Pacific, suitable conditions for large dilution and ventilation of air pollutants. For the highest AOD cases, however, the north-south pressure dipole was not strengthened much, therefore zonal advection seems relatively weaker, probably inducing the better conditions for the accumulation of airborne aerosols. This contrasting pattern is found consistently for all sites, showing that LRTT

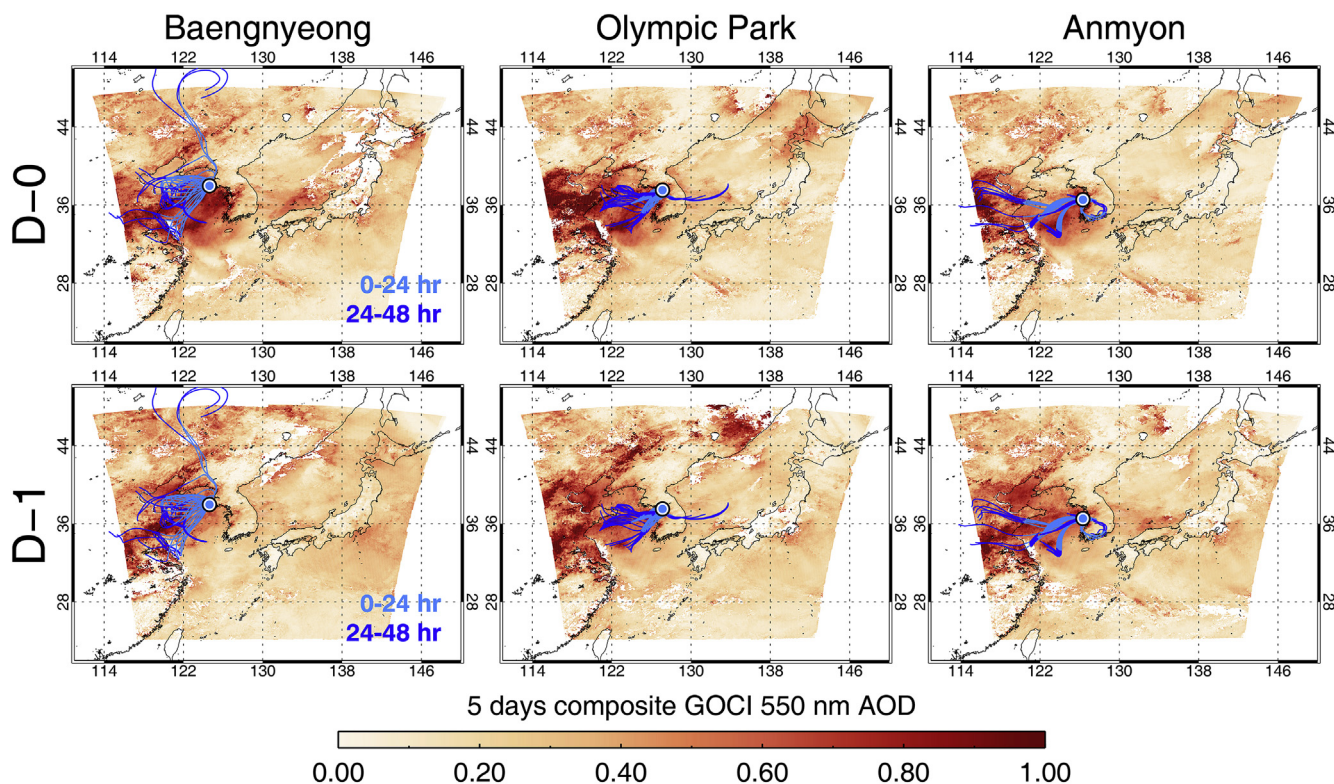


Fig. 8. GOCI 550 nm AOD pattern and 2-day back-trajectories for the 5 days of the highest AODs at Baengnyeong (left), Olympic Park (middle), and Anmyon (right). D-0 cases (top) and D-1 cases (bottom). Reddish brown colours indicate the extent of AOD. Cyan and blue colours imply the back-trajectory patterns for the period of 0–24 h and 24–48 h before the arrival, respectively. Since GOCI observations are available from 0 to 7 UTC, back-trajectories are selected for those time slots. (For interpretation of the references to colour in this figure legend, the reader is referred to the Web version of this article.)

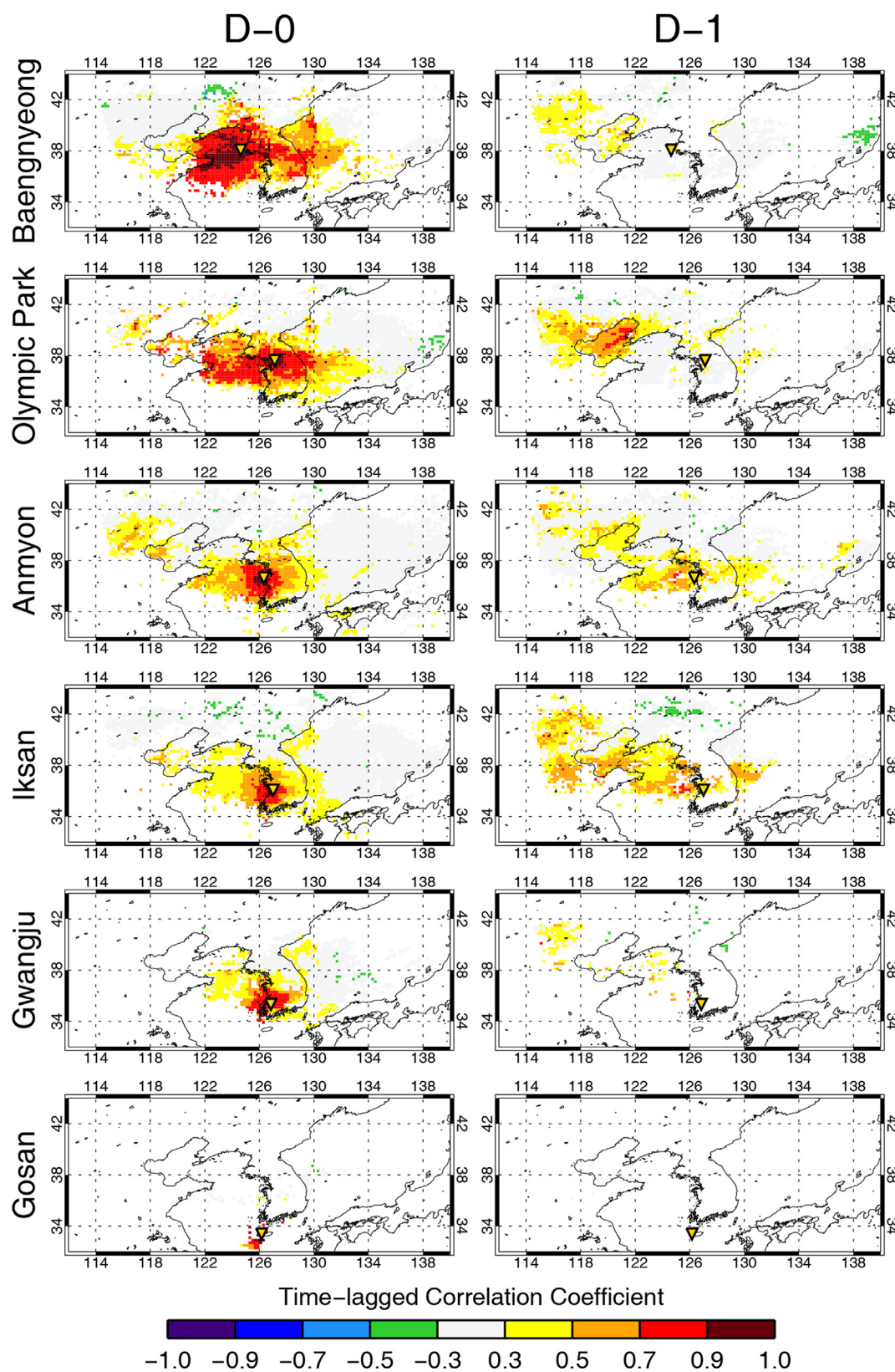


Fig. 9. Pixel-to-pixel correlations of GOCI 550 nm AODs (i.e., correlations of AODs between the pixel including the target AERONET site and all other pixels) for the whole KORUS-AQ campaign at Baengnyeong, Olympic Park, Anmyon, Iksan, Gwangju, and Gosan sites. D-0 cases (pixel to pixel correlation on the same date) and D-1 cases (correlation of target pixel to other pixels for a day before) are compared.

pattern can be modulated according to the regional meteorology.

We investigated the LRTT influence on the domestic air turbidity based on selected cases showing both the highest and lowest AOD events. Based on findings so far, it seems obvious that the LRTT of polluted air masses from east-central China contributes significantly to the extremely high AOD cases in Korea. But still, it is not sure for whether this LRTT effect is the constant or occasional factor. Therefore, next we try to perform additional analyses to generalize what we found based on the extreme cases and to evaluate the impact of LRTT.

3.2. Evaluation of the influence of the long-range transboundary transport

Using geostationary satellite AOD measurements, we confirmed the LRTT of heavy aerosol plumes from east-central China when the highest AODs are detected in the Korean peninsula (Figs. 4–6). To extend this analysis, we calculate the pixel-to-pixel correlation of AODs for each individual image during the whole KORUS-AQ period. Correlations between GOCI AODs at the pixel including each target AERONET site and all other pixels are individually estimated when the number of observations exists more than 20 days which is about half of the campaign period (Fig. 9). In addition to the correlation using AOD at the same date, i.e., no time lag (D-0), correlations with considering 1-day time lag (D-1) are also calculated.

Fig. 9 shows that AODs at the Baengnyeong and Olympic Park sites have quite high correlations with AODs over the Shandong peninsula and the Yellow Sea upwind. This correlation pattern indicates that the air turbidity at Baengnyeong and Olympic Park was usually under the standing influence of LRTT from the Shandong peninsula. Namely, it is very likely that AODs at these two Korean sites become high when large aerosol concentrations are detected over the Shandong peninsula, perhaps not only for the specific cases studied. Considering a 1-day time lag, some meaningful correlations are also found near BTH region. AODs at the Anmyon, Iksan, and Gwangju sites have moderate correlations with both D-0 and D-1 AODs over the Yellow Sea, implying that the southern part of Korea is also typically under some influence of LRTT. At Gosan, however, we do not find meaningful AOD correlations over East Asia. Considering the rather large contrast of air-mass transport between the highest and lowest AOD cases at Gosan (Figs. 4, 5 and 7), it seems that Gosan may be sometimes affected by LRTT, but usually not under the LRTT influence.

These correlation results in Fig. 9 are simple but intuitive. We clearly reveal the direct effect of air-mass transport from east-central China, the Shandong peninsula in particular. One more potential influence comes from the BTH area, which some previous research suspected as a primary source affecting the air quality in Korea (e.g., Kim et al., 2017; Lee et al., 2017). Here D-1 AOD correlations are consistent with this idea. Several recent studies have indicated that the regional emission of aerosols and their precursors over the BTH has been rapidly decreasing (Krotkov et al., 2016; Wang et al., 2017). Additionally, it was reported that recently many factories and industrial facilities in Beijing have moved to the other outside regions (Wang et al., 2018). Although how much the total emission is reduced in east-central China is the most important issue related to the air quality in Korea, the spatial distribution of emission sources is also important associated with the regional sensitivity to the specific source regions as suggested in Fig. 9. If the emission decrease at one location is connected to the emission increase at the other place in China, then despite possible reductions of total emission, the impacts of LRTT effects are only partially addressed and could be still problematic in Korea.

In further analyses, we define six discrete regions over East Asia (named as R1 to R6) and try to conduct a quantitative inspection for the LRTT effect to find the dominant sources of aerosols (Fig. 10); as depicted in Fig. 10a, R1 represents the Korean peninsula, R2 represents north China and Mongolia, R3 represents east-central China including BTH and the Shandong peninsula, R4 represents southeastern China including Shanghai and the Pearl River Delta, R5 represents the region

immediately to the south of the Korean peninsula including the East China Sea, and R6 represents the region immediately to the east of the Korean peninsula including Japan. To estimate the portion of regional contribution, all 2-day (48-h) back-trajectories are individually designated to one of six regions (R1 to R6) for deciding where each back-trajectory stays the longest period for a day or 1–2 days before arrival at each target site (Fig. 10b).

As a result, the Baengnyeong site located in the most western Korea has the largest portion of back-trajectories from R3 and R2, showing that most of air masses are transported from eastern-central China. Considering the height of back-trajectories (Fig. 7), however, air-masses from the R2 region do not contain the high aerosol concentration from the surface, resulted in the weak contribution to the high AOD in Korea. Olympic Park, Anmyon, Iksan, and Gwangju shows the large portion of R3 and R2 similarly when back-trajectories are 1–2 days (25–48 h) before the arrival. But for 0–1 day before the arrival at these sites, air masses mostly stay over the local R1 region, meaning that the contribution of domestic emission can also be large even if the origin of LRTT is outside of the Korean peninsula. Gosan consistently has a large portion of back-trajectories from the R5 sector. As discussed with Fig. 9, Gosan seems to be only occasionally affected by the LRTT from east-central China.

Since interpretations based only on back-trajectories are not sufficient, the AERONET AODs are also examined by matching with the results shown in Fig. 10. For each sector of LRTT, the average AODs are calculated and compared (Table 1). In general, the highest mean AOD can be found when the back-trajectories stay mostly over the R3 and R4 regions, which is another piece of evidence to suggest the strong impact of LRTT from southeastern China. Olympic Park shows the largest AOD when back-trajectories mostly stay in the R1 region (within the Korean peninsula) during a day before arrival, which is reasonable due to the high levels of emission from the Seoul Metropolitan Area. Also, Gosan shows the largest AOD when back-trajectories comes from the Korean peninsula. Since more than 50% of the back-trajectories originated from the oceanic areas (R5 and R6), generally the Gosan site is more removed from the influence of polluted air transport, resulting in only occasional impacts of LRTT.

From Fig. 10 and Table 1, we can recognize the fact that domestic emissions cannot be neglected even for the case showing the occurrence of LRTT from east-central China. From Fig. 7, we also notice that the LRTT effect on regional air turbidity can be different according to the transport speed notwithstanding the same origin of transported air masses. Thus, it seems necessary to investigate the influence of LRTT with the consideration of travel distance in the unit time period (i.e., travel speed). For 6 target sites, therefore we compare regionally discrete AODs from R1 to R6 in terms of the transport distance for 2 days, which can be estimated from the back-trajectory information (Fig. 11). As a result, travel distances are generally short when most back-trajectories stay over R1 (Korean domestic area) as expected. For cases that back-trajectories dominantly stay in the outside of the Korean peninsula (R2 to R6), travel distances are the longest when back-trajectories mostly stay over the R2 region. If the travel distance is longer than ~1500 km in 2 days (i.e., ~750 km/day), most of LRTT occurs from and through the R2 region, and all 6 target sites consistently have quite low AODs in these cases. The R2 region has been known as a source of the Asian dust intruded to the Korean peninsula (Lee et al., 2013b, 2015). While the Asian dust transport is generally strong in early spring (Koo et al., 2016), the continental dust transport effect was weak during May and June 2016 of the KORUS-AQ campaign.

Most of 2-day LRTT cases coming from R3, R4, R5, and R6 also illustrate that AOD becomes lower on average as the travel distance increases. We explained above that the low AOD related to the transport from R2 region occurs due to the contribution of less polluted air masses above the boundary layer (Fig. 7). But back-trajectories from the R3 and R4 regions are mostly attributed to the inside of the boundary layer, strongly contributing to the Korean air quality as we noted above.

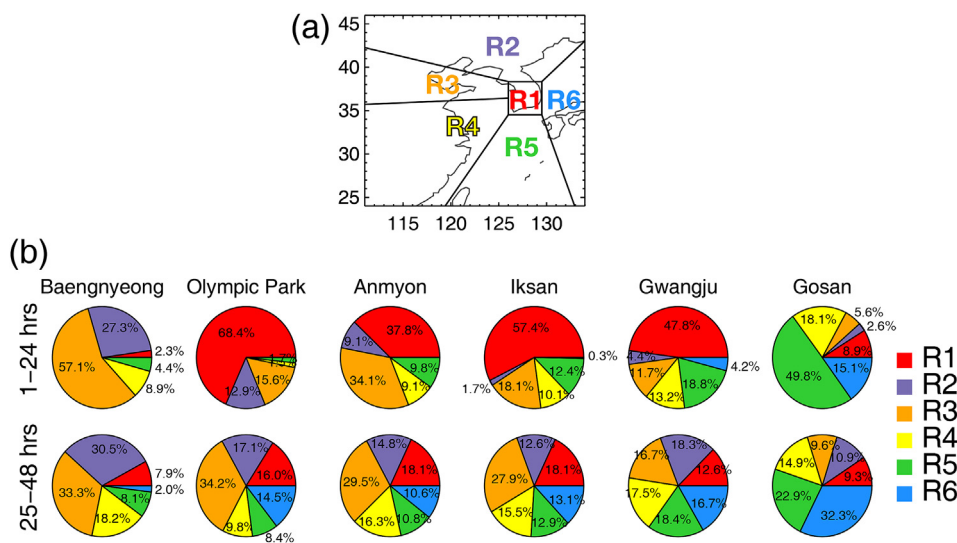


Fig. 10. (a) The six regions (R1, R2, R3, R4, R5, and R6) defined for the analysis of spatial pattern of back-trajectories. (b) The regional portion showing where (R1 to R6) back-trajectories mostly stay before arrival at Baengnyeong, Olympic Park, Anmyon, Iksan, Gwangju, and Gosan sites. The regional portions are estimated about back-trajectories for periods of 1–24 h (top) and 25–48 h (bottom) before the arrival, respectively.

Table 1

At six receptor stations (Baengnyeong, Olympic Park, Anmyon, Iksan, Gwangju, and Gosan), AERONET AODs at 550 nm are averaged and compared for all sectors (from R1 to R6) after every back-trajectory is designated to one of 6 sectors to indicate where each back-trajectory stays the longest. For this calculation, back-trajectories for the period of 1–24 h (top) and 25–48 h (bottom) before the arrival are separately considered. Numbers in parentheses represent the number of designated back-trajectories.

Region	Baengnyeong	Olympic Park	Anmyon	Iksan	Gwangju	Gosan
Mean AERONET 550 nm AOD for the case of 1–24 h						
1	0.311 (7)	0.487 (209)	0.457 (133)	0.478 (176)	0.458 (84)	0.429 (13)
2	0.216 (66)	0.305 (27)	0.175 (22)	NaN (0)	0.437 (7)	NaN (0)
3	0.289 (111)	0.373 (39)	0.328 (107)	0.420 (53)	0.212 (27)	0.255 (11)
4	0.999 (5)	NaN (0)	1.309 (18)	0.862 (27)	0.461 (15)	0.317 (40)
5	NaN (0)	NaN (1)	0.313 (19)	0.429 (25)	0.256 (13)	0.296 (33)
6	NaN (0)	NaN (0)	NaN (0)	NaN (0)	0.171 (5)	0.394 (29)
Mean AERONET 550 nm AOD for the case of 25–48 h						
1	0.299 (11)	0.519 (55)	0.417 (88)	0.570 (52)	0.379 (25)	0.560 (14)
2	0.197 (82)	0.304 (60)	0.231 (53)	0.282 (50)	0.298 (56)	0.282 (21)
3	0.330 (71)	0.535 (104)	0.375 (86)	0.598 (75)	0.446 (37)	0.311 (35)
4	0.418 (27)	0.498 (16)	0.975 (35)	0.718 (52)	0.455 (19)	0.430 (17)
5	NaN (0)	0.497 (7)	0.481 (14)	0.482 (21)	0.571 (7)	0.376 (12)
6	NaN (0)	0.291 (41)	0.267 (25)	0.320 (46)	0.424 (18)	0.203 (43)

Then this relationship between low AOD and long travel distance in 2 days (i.e., fast transport) can be interpreted in terms of the dilution or ventilation effect. In other words, AOD can be much higher under the stagnant air condition compared to the windy conditions despite the same source influence, also supported by the meteorology pattern (Fig. S14). Consequently, both the direction and speed of LRTT should be simultaneously considered for the exact evaluation of LRTT effect.

Based on the comprehensive analyses shown in Fig. 11, we find Baengnyeong and Anmyon sites, located in the western coast of the Korean peninsula, have the largest AOD when back-trajectories travels about 500–1500 km for 2 days (250–750 km/day) from east-central and southeast China (R3 and R4). If travel distances in 2 days become longer, AODs rapidly drop. Differing from both Baengnyeong and Anmyon, the Olympic Park, Iksan, and Gwangju sites show the largest AOD when the back-trajectories only move < 500 km for 2 days (< 250 km/day), mostly staying over the R1 region. Considering that Olympic Park, Iksan, and Gwangju are the urban region, the large contribution of local pollution to the high AOD looks reasonable. The interesting point is that local domestic influence can be larger than LRTT effect when the atmosphere is stagnated. This pattern does not occur in rural sites that are also partially surrounded by ocean waters such as Baengnyeong and Anmyon. In sum, usually the western part of the Korean peninsula has the high AOD when there is a moderate westerly flow. If the westerly becomes strong (i.e., fast wind), transported air masses are diluted and regional atmosphere is well

ventilated, resulting in the cleaner air condition. If the domestic air condition becomes stagnant, however, then urban sites can have higher AOD patterns due to the accumulation of locally emitted pollutants, particularly urban industrial aerosols. Thus, the investigation of domestic aerosol emissions is also important in addition to the evaluation of LRTT influences.

4. Summary and conclusion

This study investigated the influence of LRTT on the extent of aerosol pollution in the Korean peninsula. In addition to the typical back-trajectory analysis with ground-based AOD measurements, we utilized AODs from the geostationary satellite measurement, which can detect the progression and evolution of aerosol plumes between countries. Our study confirmed that the back-trajectory patterns for the high polluted case of receptor sites well follow the real movement of aerosol plumes from east-central China including the Shandong peninsula. Some contributions from the BTH region are also identified considering 1-day time lag. When the severe aerosol plume is carried into the Korean peninsula, air turbidity becomes enhanced > 200% over the pathway of LRTT comparing to the mean situation. Travel speed of air-masses also looks important for the evaluation of LRTT impact. Westerly from the source region shows the largest impact when the travel speed is about 250–750 km/day, but the local emission impact is larger for cases < 250 km/day.

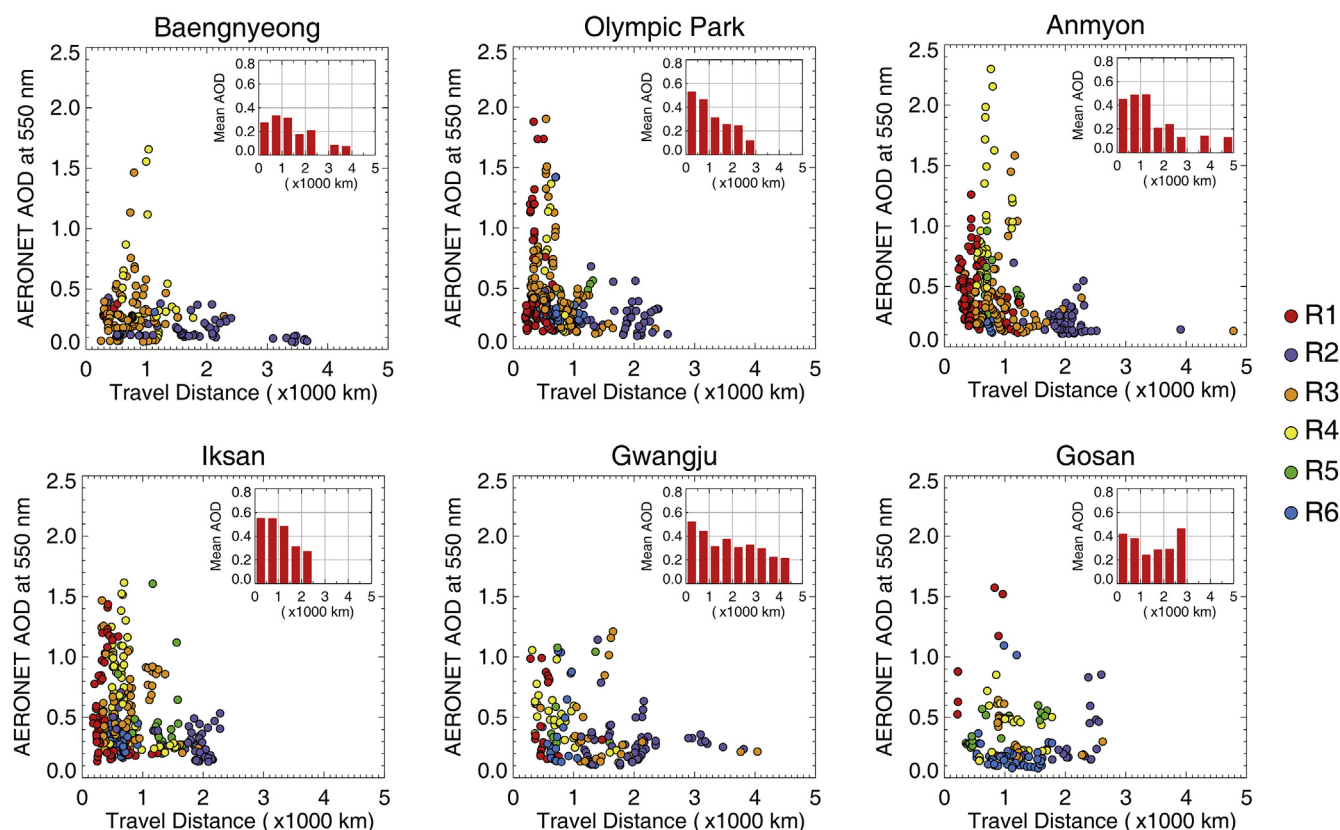


Fig. 11. Relationship between AERONET 550 nm AODs and the travel distance of 2-day back-trajectories arrived at the Baengnyeong, Olympic Park, Anmyon, Iksan, Gwangju, and Gosan sites. Coloured dots indicate where back-trajectories stay the longest (R1 to R6). Small bar plots in the panels show the mean AODs estimated for each range of travel distance in 2 days, with 500 km intervals.

In the past, LRTT analysis based only on the back-trajectory analysis has a difficulty to show the movement of real pollutants. Our study, however, reveals that the combination of back-trajectory and geostationary satellite monitoring well illuminates the pattern of aerosol plume transport from the outside, improving the reliability of the back-trajectory analysis. Investigations of travel speed and height of air-masses are other useful approaches for the diagnosis of LRTT effect, showing a slow advection in the boundary layer has the larger contribution compared with the fast transport above the boundary layer. Despite these findings, further efforts will be necessary for better understanding. For example, the relay effect of aerosol (Miao et al., 2017) cannot be negligible for the evaluation of transport effect. Consideration of relay effect will be able to suggest the additional idea about the polluted cases not clearly explained by LRTT pattern so far.

All findings in this study clarified that the emissions in east-central China substantially influence the aerosol pollution in the Korean peninsula. In particular, air quality conditions between the Shandong peninsula and the northwestern area of South Korea look strongly connected with each other. We confirmed that top-ranked aerosol pollution events in South Korea are dominantly affected by the LRTT from east-central China. For the reduction of serious air turbidity problems in South Korea, therefore, the national cooperation between China and Korea will be necessary. It is recommended that more scientific studies are conducted across South Korea and that science collaborations between the two countries are pursued to address this serious issue.

Declaration of interests

The authors declare that they have no known competing financial interests or personal relationships that could have appeared to

influence the work reported in this paper.

The authors declare the following financial interests/personal relationships which may be considered as potential competing interests:

Acknowledgements

This subject was funded by Korea Ministry of Environment (MOE) as the Public Technology Program based on Environmental Policy (2017000160001). We thank all the AERONET principal investigators and their staff for establishing and maintaining the 19 AERONET sites used in this study. We also appreciate the contribution of Korea U.S.-Air Quality (KORUS-AQ) campaign (<https://doi.org/10.567/Suborbital/KORUSAQ/DATA01>). We also thank the MODIS science team for providing valuable data for this research. The authors gratefully acknowledge the NOAA Air Resources Laboratory (ARL) for the provision of the HYSPLIT transport and dispersion model and READY website (<http://www.ready.noaa.gov>) used in this publication. The authors would like to thank ECMWF and NCEP/NCAR for providing meteorological reanalysis data. MC's work was undertaken as a private enterprise and not in the author's capacity as an employee of the Jet Propulsion Laboratory, California Institute of Technology.

Appendix A. Supplementary data

Supplementary data to this article can be found online at <https://doi.org/10.1016/j.atmosenv.2019.02.020>.

References

- Choi, J.-K., Park, Y.J., Ahn, J.H., Lim, H.-S., Eom, J., Ryu, J.-H., 2012. GOCI, the world's first geostationary ocean color observation satellite, for the monitoring of temporal variability in coastal water turbidity. *J. Geophys. Res.-Oceans*. 117, C09004. <https://doi.org/10.1029/2011JC007401>

- doi.org/10.1029/2012jc008046.
- Choi, M., Kim, J., Lee, J., Kim, M., Park, Y.-J., Jeong, U., Kim, W., Hong, H., Holben, B.N., Eck, T.F., Song, C.H., Lim, J.-H., Song, C.-K., 2016. GOCI Yonsei aerosol retrieval (YAER) algorithm and validation during the DRAGON-NE Asia 2012 campaign. *Atmos. Meas. Tech.* 9 (3), 1377–1398. <https://doi.org/10.5194/amt-9-1377-2016>.
- Choi, M., Kim, J., Lee, J., Kim, M., Park, Y.-J., Holben, B.N., Eck, T.F., Li, Z., Song, C.H., 2018. GOCI Yonsei aerosol retrieval version 2 products: an improved algorithm and error analysis with uncertainty estimation from 5-year validation over East Asia. *Atmos. Meas. Tech.* 11 (1), 385–408. <https://doi.org/10.5194/amt-11-385-2018>.
- Choi, S.H., Ghim, Y.S., Chang, Y.S., Jung, K., 2014. Behavior of particulate matter during high concentration episodes in Seoul. *Environ. Sci. Pollut. Res.* 21 (9), 5972–5982. <https://doi.org/10.1007/s11356-014-2555-y>.
- Cooper, O.R., Forster, C., Parrish, D., Trainer, M., Dunlea, E., Ryerson, T., Hübner, G., Fehsenfeld, F., Nicks, D., Holloway, J., de Gouw, J., Warneke, C., Roberts, J.M., Flocke, F., Moody, J., 2004. A case study of transpacific warm conveyor belt transport: influence of merging airstreams on trace gas import to North America. *J. Geophys. Res. Atmos.* 109, D23S08. <https://doi.org/10.1029/2003jd003624>.
- Eck, T.F., Holben, B.N., Reid, J.S., Dubovik, O., Smirnov, A., O'Neill, N.T., Slutsker, I., Kinne, S., 1999. Wavelength dependence of the optical depth of biomass burning, urban, and desert dust aerosols. *J. Geophys. Res. Atmos.* 104 (D24), 31333–31349. <https://doi.org/10.1029/1999jd900923>.
- Eck, T.F., Holben, B.N., Reid, J.S., Xian, P., Giles, D.M., Sinyuk, A., Smirnov, A., Schafer, J.S., Slutsker, I., Kim, J., Koo, J.H., Choi, M., Kim, K.C., Sano, I., Arola, A., Sayer, A.M., Levy, R.C., Munchak, L.A., O'Neill, N.T., Lyapustin, A., Hsu, N.C., Randles, C.A., Da Silva, A.M., Buchard, V., Govindaraju, R.C., Hyer, E., Crawford, J.H., Wang, P., Xia, X., 2018. Observations of the interaction and transport of fine mode aerosols with cloud and/or fog in northeast Asia from aerosol robotic network and satellite remote sensing. *J. Geophys. Res. Atmos.* 123 (10), 5560–5587. <https://doi.org/10.1029/2018jd028313>.
- Eguchi, K., Uno, I., Yumimoto, K., Takemura, T., Shimizu, A., Sugimoto, N., Liu, Z., 2009. Trans-pacific dust transport: integrated analysis of NASA/CALIPSO and a global aerosol transport model. *Atmos. Chem. Phys.* 9, 3137–3145.
- Giles, D.M., Sinyuk, A., Sorokin, M.G., Schafer, J.S., Smirnov, A., Slutsker, I., Eck, T.F., Holben, B.N., Lewis, J.R., Campbell, J.R., Welton, E.J., Korkin, S.V., Lyapustin, A.I., 2019. Advancements in the Aerosol Robotic Network (AERONET) Version 3 database – automated near-real-time quality control algorithm with improved cloud screening for Sun photometer aerosol optical depth (AOD) measurements. *Atmos. Meas. Tech.* 12, 169–209. <https://doi.org/10.5194/amt-12-169-2019>.
- Guo, J., Zhang, X., Cao, C., Che, H., Liu, H., Gupta, P., Zhang, H., Xu, M., Li, X., 2010. Monitoring haze episodes over the Yellow Sea by combining multisensor measurements. *Int. J. Remote Sens.* 31 (17–18), 4743–4755. <https://doi.org/10.1080/01431161.2010.485213>.
- Guo, J., Lou, M., Miao, Y., Wang, Y., Zeng, Z., Liu, H., He, J., Xu, H., Wang, F., Min, M., Zhai, P., 2017. Trans-Pacific transport of dust aerosols from East Asia: insights gained from multiple observations and modeling. *Environ. Pollut.* 230, 1030–1039. <https://doi.org/10.1016/j.envpol.2017.07.062>.
- He, Z., Kim, Y.J., Ogunjobi, K.O., Hong, C.S., 2003. Characteristics of PM_{2.5} species and long-range transport of air masses at Taejeon background station, South Korea. *Atmos. Environ.* 37, 219–230.
- Heo, J.-B., Hopke, P.K., Yi, S.-M., 2009. Source apportionment of PM_{2.5} in Seoul, Korea. *Atmos. Chem. Phys.* 9, 4957–4971.
- Holben, B.N., Eck, T.F., Slutsker, I., Tanre, D., Buis, J.P., Setzer, A., Vermote, E., Reagan, J.A., Kaufman, Y.J., Nakajima, T., Lavenut, F., Jankowiak, I., Smirnov, A., 1998. AERONET – a federated instrument network and data archive for aerosol characterization. *Remote Sens. Environ.* 66 (1), 1–16.
- Jeong, U., Kim, J., Lee, H., Jung, J., Kim, Y.J., Song, C.H., Koo, J.H., 2011. Estimation of the contributions of long range transported aerosol in East Asia to carbonaceous aerosol and PM concentrations in Seoul, Korea using highly time resolved measurements: a PSCF model approach. *J. Environ. Monit.* 13 (7), 1905–1918. <https://doi.org/10.1039/c0em00659a>.
- Jeong, U., Kim, J., Lee, H., Lee, Y.G., 2017. Assessing the effect of long-range pollutant transportation on air quality in Seoul using the conditional potential source contribution function method. *Atmos. Environ.* 150, 33–44. <https://doi.org/10.1016/j.atmosenv.2016.11.017>.
- Kim, B.-U., Bae, C., Kim, H.C., Kim, E., Kim, S., 2017. Spatially and chemically resolved source apportionment analysis: case study of high particulate matter event. *Atmos. Environ.* 162, 55–70. <https://doi.org/10.1016/j.atmosenv.2017.05.006>.
- Kim, J., 2008. Transport routes and source regions of Asian dust observed in Korea during the past 40 years (1965–2004). *Atmos. Environ.* 42 (19), 4778–4789. <https://doi.org/10.1016/j.atmosenv.2008.01.040>.
- Kim, J.Y., Kim, S.-W., Ghim, Y.S., Song, C.H., Yoon, S.-C., 2012. Aerosol properties at gosan in Korea during two pollution episodes caused by contrasting weather conditions. *Asia-Pac. J. Atmos. Sci.* 48 (1), 25–33. <https://doi.org/10.1007/s13143-012-0003-9>.
- Kim, M., Kim, J., Jeong, U., Kim, W., Hong, H., Holben, B., Eck, T.F., Lim, J.H., Song, C.K., Lee, S., Chung, C.Y., 2016. Aerosol optical properties derived from the DRAGON-NE Asia campaign, and implications for a single-channel algorithm to retrieve aerosol optical depth in spring from Meteorological Imager (MI) on-board the Communication, Ocean, and Meteorological Satellite (COMS). *Atmos. Chem. Phys.* 16 (3), 1789–1808. <https://doi.org/10.5194/acp-16-1789-2016>.
- Kim, S.-W., Yoon, S.-C., Kim, J., Kim, S.-Y., 2007. Seasonal and monthly variations of columnar aerosol optical properties over east Asia determined from multi-year MODIS, LIDAR, and AERONET Sun/sky radiometer measurements. *Atmos. Environ.* 41 (8), 1634–1651. <https://doi.org/10.1016/j.atmosenv.2006.10.044>.
- Kim, Y.J., Woo, J.-H., Ma, Y.-I., Kim, S., Nam, J.S., Sung, H., Choi, K.-C., Seo, J., Kim, J.S., Yang, C.-H., 2009. Chemical characteristics of long-range transport aerosol at background sites in Korea. *Atmos. Environ.* 43 (34), 5556–5566. <https://doi.org/10.1016/j.atmosenv.2009.03.062>.
- Koo, J.H., 2008. Optical Properties of Aerosol in a Megacity, Seoul from Ground-Based and Satellite Measurements. MS thesis. Department of Atmospheric Sciences, Yonsei University.
- Koo, J.-H., Kim, J., Kim, J., Lee, H., Noh, Y.M., Lee, Y.G., 2016. Springtime trans-Pacific transport of Asian pollutants characterized by the Western Pacific (WP) pattern. *Atmos. Environ.* 147, 166–177. <https://doi.org/10.1016/j.atmosenv.2016.10.007>.
- Krotkov, N.A., McLinden, C.A., Li, C., Lamsal, L.N., Celarier, E.A., Marchenko, S.V., Swartz, W.H., Bucsela, E.J., Joiner, J., Duncan, B.N., Boersma, K.F., Veefkind, J.P., Levett, P.F., Fioletov, V.E., Dickerson, R.R., He, H., Lu, Z., Streets, D.G., 2016. Aura OMI observations of regional SO₂ and NO₂ pollution changes from 2005 to 2015. *Atmos. Chem. Phys.* 16 (7), 4605–4629. <https://doi.org/10.5194/acp-16-4605-2016>.
- Lee, H.-J., Kim, J.E., Cha, J.W., Song, S., Ryoo, S.-B., Kim, Y.P., 2018a. Characteristics of long-lasting haze episodes observed in Seoul, South Korea, for 2009–2014. *Theor. Appl. Climatol.* <https://doi.org/10.1007/s00704-018-2415-7>.
- Lee, H.M., Park, R.J., Henze, D.K., Lee, S., Shim, C., Shin, H.J., Moon, K.J., Woo, J.H., 2017. PM_{2.5} source attribution for Seoul in May from 2009 to 2013 using GEOS-Chem and its adjoint model. *Environ. Pollut.* 221, 377–384. <https://doi.org/10.1016/j.envpol.2016.11.088>.
- Lee, K.H., Kim, Y.J., Kim, M.J., 2006. Characteristics of aerosol observed during two severe haze events over Korea in June and October 2004. *Atmos. Environ.* 40 (27), 5146–5155. <https://doi.org/10.1016/j.atmosenv.2006.03.050>.
- Lee, S., Ho, C.-H., Choi, Y.-S., 2011. High-PM₁₀ concentration episodes in Seoul, Korea: background sources and related meteorological conditions. *Atmos. Environ.* 45 (39), 7240–7247. <https://doi.org/10.1016/j.atmosenv.2011.08.071>.
- Lee, S., Ho, C.-H., Lee, Y.G., Choi, H.-J., Song, C.-K., 2013a. Influence of transboundary air pollutants from China on the high-PM₁₀ episode in Seoul, Korea for the period October 16–20, 2008. *Atmos. Environ.* 77, 430–439. <https://doi.org/10.1016/j.atmosenv.2013.05.006>.
- Lee, S., Hong, J., Cho, Y., Choi, M., Kim, J., Park, S.S., Ahn, J.-Y., Kim, S.-K., Moon, K.-J., Eck, T.F., Holben, B.N., Koo, J.-H., 2018b. Characteristics of classified aerosol types in South Korea during the MAPS-seoul campaign. *Aerosol Air Qual. Res.* 18 (9), 2195–2206. <https://doi.org/10.4209/aaqr.2017.11.0474>.
- Lee, Y.G., Ho, C.-H., Kim, J.-H., Kim, J., 2015. Quiescence of Asian dust events in South Korea and Japan during 2012 spring: dust outbreaks and transports. *Atmos. Environ.* 114, 92–101. <https://doi.org/10.1016/j.atmosenv.2015.05.035>.
- Lee, Y.G., Ho, C.-H., Kim, J., Kim, J., 2013b. Potential impacts of northeastern Eurasian snow cover on generation of dust storms in northwestern China during spring. *Clim. Dyn.* 41 (3–4), 721–733. <https://doi.org/10.1007/s00382-012-1522-x>.
- Lim, H., Choi, M., Kim, J., Kasai, Y., Chan, P., 2018. AHI/Himawari-8 Yonsei aerosol retrieval (YAER): algorithm, validation and merged products. *Rem. Sens.* 10 (5). <https://doi.org/10.3390/rs10050699>.
- Miao, Y., Guo, J., Liu, S., Liu, H., Zhang, G., Yan, Y., He, J., 2017. Relay transport of aerosols to Beijing-Tianjin-Hebei region by multi-scale atmospheric circulations. *Atmos. Environ.* 165, 35–45. <https://doi.org/10.1016/j.atmosenv.2017.06.032>.
- Naeger, A.R., Gupta, P., Zavadsky, B.T., McGrath, K.M., 2016. Monitoring and tracking the trans-Pacific transport of aerosols using multi-satellite aerosol optical depth composites. *Atmos. Meas. Tech.* 9 (6), 2463–2482. <https://doi.org/10.5194/amt-9-2463-2016>.
- Nakajima, T., Tonna, G., Rao, R., Boi, P., Kaufman, Y., Holben, B., 1996. Use of sky brightness measurements from ground for remote sensing of particulate polydispersions. *Appl. Optic.* 35 (15), 2672–2686.
- Oh, H.-R., Ho, C.-H., Kim, J., Chen, D., Lee, S., Choi, Y.-S., Chang, L.-S., Song, C.-K., 2015. Long-range transport of air pollutants originating in China: a possible major cause of multi-day high-PM₁₀ episodes during cold season in Seoul, Korea. *Atmos. Environ.* 109, 23–30. <https://doi.org/10.1016/j.atmosenv.2015.03.005>.
- Park, M.E., Song, C.H., Park, R.S., Lee, J., Kim, J., Lee, S., Woo, J.H., Carmichael, G.R., Eck, T.F., Holben, B.N., Lee, S.S., Song, C.K., Hong, Y.D., 2014. New approach to monitor transboundary particulate pollution over Northeast Asia. *Atmos. Chem. Phys.* 14 (2), 659–674. <https://doi.org/10.5194/acp-14-659-2014>.
- Sahu, L.K., Kondo, Y., Miyazaki, Y., Kuwata, M., Koike, M., Takegawa, N., Tanimoto, H., Matsueda, H., Yoon, S.C., Kim, Y.J., 2009. Anthropogenic aerosols observed in Asian continental outflow at Jeju Island, Korea, in spring 2005. *J. Geophys. Res.* 114 (D3). <https://doi.org/10.1029/2008jd010306>.
- Saide, P.E., Kim, J., Song, C.H., Choi, M., Cheng, Y., Carmichael, G.R., 2014. Assimilation of next generation geostationary aerosol optical depth retrievals to improve air quality simulations. *Geophys. Res. Lett.* 41 (24), 9188–9196. <https://doi.org/10.1002/2014gl026089>.
- Schmeisser, L., Andrews, E., Ogren, J.A., Sheridan, P., Jefferson, A., Sharma, S., Kim, J.E., Sherman, J.P., Sorribas, M., Kalapov, I., Arsov, T., Angelov, C., Mayol-Bracero, O.L., Labuschagne, C., Kim, S.-W., Hoffer, A., Lin, N.-H., Chia, H.-P., Bergin, M., Sun, J., Liu, P., Wu, H., 2017. Classifying aerosol type using in situ surface spectral aerosol optical properties. *Atmos. Chem. Phys.* 17 (19), 12097–12120. <https://doi.org/10.5194/acp-17-12097-2017>.
- Seo, J., Kim, J.Y., Youn, D., Lee, J.Y., Kim, H., Lim, Y.B., Kim, Y., Jin, H.C., 2017. On the midday haze in the Asian continental outflow: the important role of synoptic conditions combined with regional and local sources. *Atmos. Chem. Phys.* 17 (15), 9311–9332. <https://doi.org/10.5194/acp-17-9311-2017>.
- Smirnov, A., Holben, B.N., Eck, T.F., Dubovik, O., Slutsker, I., 2000. Cloud screening and quality control algorithms for the AERONET data base. *Remote Sens. Environ.* 73 (3), 337–349.
- Stein, A.F., Draxler, R.R., Rolph, G.D., Stunder, B.J.B., Cohen, M.D., Ngan, F., 2015. NOAA's HYSPLIT atmospheric transport and dispersion modeling system. *Bull. Am. Meteorol. Soc.* 96 (12), 2059–2077. <https://doi.org/10.1175/bams-d-14-00110>.
- Wang, J., Zhao, B., Wang, S., Yang, F., Xing, J., Morawski, L., Ding, A., Kulmala, M.,

- Kerminen, V.M., Kujansuu, J., Wang, Z., Ding, D., Zhang, X., Wang, H., Tian, M., Petaja, T., Jiang, J., Hao, J., 2017. Particulate matter pollution over China and the effects of control policies. *Sci. Total Environ.* 584–585, 426–447. <https://doi.org/10.1016/j.scitotenv.2017.01.027>.
- Wang, L., Zhang, F., Pilot, E., Yu, J., Nie, C., Holdaway, J., Yang, L., Li, Y., Wang, W., Vardoulakis, S., Krafft, T., 2018. Taking action on air pollution control in the beijing-tianjin-hebei (BTH) region: progress, challenges and opportunities. *Int. J. Environ. Res. Public Health* 15 (2). <https://doi.org/10.3390/ijerph15020306>.
- Yoo, J.M., Jeong, M.J., Kim, D., Stockwell, W.R., Yang, J.H., Shin, H.W., Lee, M.I., Song, C.K., Lee, S.D., 2015. Spatiotemporal variations of air pollutants (O_3 , NO_2 , SO_2 , CO, PM_{10} , and VOCs) with land-use types. *Atmos. Chem. Phys.* 15 (18), 10857–10885. <https://doi.org/10.5194/acp-15-10857-2015>.
- Yu, H., Remer, L.A., Chin, M., Bian, H., Kleidman, R.G., Diehl, T., 2008. A satellite-based assessment of transpacific transport of pollution aerosol. *J. Geophys. Res.* 113 (D14). <https://doi.org/10.1029/2007jd009349>.
- Yumimoto, K., Eguchi, K., Uno, I., Takemura, T., Liu, Z., Shimizu, A., Sugimoto, N., Strawbridge, K., 2010. Summertime trans-Pacific transport of Asian dust. *Geophys. Res. Lett.* 37, L18815. <https://doi.org/10.1029/2010GL043995>.